Shielding and Crystal Fields at Rare-Earth Ions

GERALD BURNS
Thomas J. Watson Research Center, International Business Machines Corporation, Yorktown Heights, New York

(Received June 27, 1962)

Several aspects of the crystal field problem of rare-earth ions in ionic solids are discussed. In particular, three problems are considered. (1) A calculation is performed to determine to what extent the $5s^2p^6$ electrons shield the $4f$ electrons from the crystal field. The shielding is small ($<10\%$) and unimportant compared to the many other uncertainties in crystal field calculations. The calculation was carried out by considering the crystal field, $\Sigma B_n{}^m r^n, Y_n{}^m$, as a perturbation on the $5s^2$ and $5p^6$ state. The excited state wave functions are calculated and the extra potential, $\Sigma B_n{}^m Y_n{}^m F_{n,m}(r)$, due to the distorted charge distribution is compared to crystal potential. (2) The reason as to why the rare-earth ions effectively see smaller crystal fields than the iron series ions is considered by performing the lattice sums in several typical lattices so that the $B_n{}^m$ coefficients could be compared. One observes that the crystal field to spin-orbit coupling ratio is considerably larger in the iron series ions than for the rare-earth ions for straightforward reasons (the ion series ions have $B_n{}^m \approx 3$ to 10 times larger, $\langle r_n \rangle \approx 2$ times larger and spin-orbit coupling constants $\approx 1/2$ as large as the rare-earth ions). Thus, the difference in behavior between these two groups of ions comes about for straightforward reasons without resorting to shielding. (3) The calculated crystal field parameters, $\langle r_n \rangle B_n{}^m = V_n{}^m$, for the rare-earth ions are compared with those obtained by fitting optical levels. A discussion of the problems involved in calculating the lattice sums ($B_n{}^m$) is given and one can see why detailed agreement is not expected. The calculated $V_n{}^m$ for $n=4$ and 6 are reasonable but smaller than those obtained from the optical data. Little can be said for the $n=2$ terms because of the uncertainties involved in the lattice sums.

INTRODUCTION

IT has been known for a long time that the electron paramagnetism of rare-earth ions in insulating crystals is very different from that of the iron series ions. The rare-earth ions essentially behave as though they are in the gas phase. That is, the effect of the crystal field is small compared to spin-orbit interactions.[1] Thus, J is a good quantum number ($\mathbf{J}=\mathbf{L}+\mathbf{S}$). On the other hand, the iron series ions behave as though the orbital angular momentum is zero. Treating the crystal field as large compared to the spin-orbit interaction one can obtain this quenching of orbital angular momentum. The reason for this difference in behavior between the rare-earth ions and iron series ions is often stated as follows: "The $4f$ shell, which is responsible for paramagnetism in the rare earths, is shielded from the crystal fields by the outer $5s^2p^6$ electrons while in the iron series ions the $3d$ electrons are the outermost electrons and are thus not shielded and see the very strong crystal fields."

This statement is examined. A calculation is made of the magnitude of this shielding in rare-earth ions and it is found to be unimportant. Thus, the difference between the rare-earth ion behavior and the iron series ions is not due to the fact that the outer electron shells shield the $4f$ electrons from the crystal fields. Then a calculation of the crystal fields in several host lattices that typically accept rare-earth ions and several host lattices that accept iron series ions was performed [i.e., the crystal field is written in the usual form[1] $V_{\text{cry}}=\sum B_n{}^m r^n Y_n{}^m(\theta,\phi)$ and the $B_n{}^m$'s, which are lattice sums, are calculated]. In the iron series lattices the crystal fields are as much as ten times larger than the rare-earth type lattices. Also, the crystal field splittings are determined by the product $\langle r^n \rangle B_n{}^m$, where $\langle r^n \rangle$ is the expectation value of r^n over the $3d$ or $4f$ wave function, and $\langle r^n \rangle$ for the $3d$ iron series ions is typically two times larger than for the $4f$ rare-earth ions. Lastly, the spin-orbit coupling parameter for the iron series ions is at least two times smaller than that for the rare-earth ions. Thus, without resorting to shielding, one observes that the difference in behavior between the iron series and the rare-earth ions comes about in a straightforward manner.

SHIELDING

In this section the shielding calculation is discussed. A simple perturbation calculation is performed in which the crystal field, $B_n{}^m r^n Y_n{}^m(\theta,\phi)$, is the perturbing Hamiltonian, H_1.

The ground state $5s$ or $5p$ wave function, ψ_0, has matrix elements with only certain excited states for certain terms in the crystal field. The symmetry of these excited states is precisely the correct form so that one can write an additional potential energy for electrons about the origin (the rare-earth ion) as $B_n{}^m Y_n{}^m(\theta,\phi)F_{n,m}(r)$. Then the $4f$ electrons on the rare-earth ion see a potential energy $B_n{}^m Y_n{}^m[r^n+F_{n,m}(r)]$. The relative magnitude and sign of the expectation value of r^n and[2] $F(r)$ over the $4f$ wave function will determine the magnitude of the shielding or antishielding of the crystal field.

To be more specific consider, for example, the $B_4{}^0 r^4 Y_4{}^0$ term. This will connect the $5s$ ground-state wave function to excited-state wave functions that have g orbital angular momentum (i.e., $l=4$). Thus, the wave func-

[1] For general references, see B. Bleaney and K. W. H. Stevens, Repts. Progr. Phys. **16**, 108 (1953); and W. Low, in *Solid State Physics*, edited by F. Seitz and D. Turnbull (Academic Press Inc., New York, 1960), Suppl. 2.

[2] For the sake of brevity some of the θ, ϕ, and subscripts will be left out. Thus, $F(r)=F_{n,m}(r)$, $Y_n{}^m=Y_n{}^m(\theta\phi)$, and $P_n{}^m=P_n{}^m(\cos\theta)$, etc.

tion is

$$\psi=\psi_{5s}+\sum_{\text{all}\,g}\frac{\langle 5s|B_4{}^0r^4Y_4{}^0|g\rangle}{E_{5s}-E_g}\psi_g=\psi_{5s}+\psi_1. \quad (1)$$

In a similar manner the $B_4{}^0$ term will connect p states to f and h states (i.e., $p\rightarrow f$ and $p\rightarrow h$). Then one can compute the electrostatic potential due to this new wave function from[3]

$$V(r,\theta,\phi)=\sum_{n=0}^{\infty}\sum_{m=-n}^{+n}\frac{(n-|m|)!}{(n+|m|)!}P_n{}^m(\cos\theta)e^{-im\phi}$$
$$\times\left[\frac{1}{r^{n+1}}\int_0^r r_i{}^n\rho_{n,m}(r_i)dr_i+r^n\int_r^{\infty}\frac{\rho_{n,m}(r_i)}{r_i{}^{n+1}}dr_i\right], \quad (2)$$

where

$$\rho_{n,m}(r)=\int\rho(r\theta\phi)P_n{}^m(\cos\theta)e^{im\phi}r^2\sin\theta d\theta d\phi, \quad (3)$$

$\rho(r\theta\phi)$ being the charge density $\psi^*\psi$. Now, for the example of $s\rightarrow g$, the lowest order term contributing to Eq. (2) is $2\psi_{5s}\psi_1$.

However, Eq. (1) is really of little use for this type of problem since one does not know the radial wave functions of the g (excited) states. The excited state wave function, ψ_1, must be found by a different method. The method used here is the same as has successfully been employed by Sternheimer[4] in considering similar types of problems. ψ_1 is obtained by solving the first perturbed Schrödinger equation

$$(H_0-E_0)\psi_1=-(H_1-E_1)\psi_0, \quad (4)$$

where the symbols have their usual meaning.[5] In a great many cases $E_1=0$. Then the radial form of Eq. (4), where u_1' and u_0' are r times the radial part of the respective wave functions and l' is the orbital angular momentum of the excited state (0 for s state, 1 for p state, 4 for g state, etc.), is

$$\left[-\frac{d^2}{dr^2}+\frac{l'(l'+1)}{r^2}+(V_0-E_0)\right]u_1'=-H_1u_0'. \quad (5)$$

The hard part of the problem is thus reduced to solving an ordinary differential, Eq. (5), for the radial part of the perturbed wave function. The unperturbed wave functions that are used are those calculated by Ridley[6] for $_{59}Pr^{+3}$ ($4f^25s^2p^6$) and $_{69}Tm^{+3}$ ($4f^{12}5s^2p^6$). They are calculated without exchange terms and are listed in the usual tabular form which gives u_0' values at fairly uniform separations δ in r. It is thus convenient to solve Eq. (5) by using (l is the orbital angular momentum of the ground state)

$$(V_0-E_0)=\frac{1}{u_0'}\left[\frac{d^2}{dr^2}-\frac{l(l+1)}{r^2}\right]u_0' \quad (6)$$

and

$$\frac{d^2u_1'}{dr^2}=\frac{u_1'(r+\delta)-2u_1'(r)+u_1'(r-\delta)}{\delta^2} \quad (7)$$

to obtain

$$u_1'(r+\delta)=u_1'(r)\left\{2+\delta^2\left[\frac{l'(l'+1)-l(l+1)}{r^2}\right.\right.$$
$$\left.\left.+\frac{d^2u_0'(r)/dr^2}{u_0'(r)}-\frac{H_1(r)u_0'(r)}{u_1'(r)}\right]\right\}-u_1'(r-\delta). \quad (8)$$

This equation is convenient for a computer (an IBM 7090 was used) and it is solved by starting the solution with $u_1'(r-\delta)$ equal to zero at the origin and $u_1'(r)$ is varied until u_1' behaves properly at infinity. In practice, solutions of (8) are used that diverge to $+\infty$ or $-\infty$ but the difference between the solutions over the region of interest could be made negligibly small. This method of solution has been previously used and found to give good results.[7]

The angular part of the excited-state wave function must also be known so that Eq. (3) can be solved. This type of determination has also been previously used[4] and will simply be outlined here. One can take for the $5s$ the form

$$u_0=u_0'/\sqrt{2}, \quad (9)$$

where $u_0\equiv r\psi_0$, i.e., r times the total wave function where u_0' is the radial part of u_0. Then the $B_4{}^0$ type perturbation is of the form $P_4{}^0(\cos\theta)$ so the right-hand side of Eq. (4) is of the form $P_4{}^0(\cos\theta)/\sqrt{2}$. Thus, the excited-state, g, wave function can be taken to have the form

$$u_1=P_4{}^0(\cos\theta)/\sqrt{2}$$
$$u_1'=(8\sqrt{2})^{-1}(35\cos^4\theta-30\cos^2\theta+3)u_1', \quad (10)$$

where u_1' must be obtained from Eq. (8) ($l'=4$ and $l=0$ for this particular case). Thus, $\rho_{n,m}(r)$ in Eq. (3) can readily be obtained, i.e.,

$$\rho_{4,0}(r)=4\int\left(\frac{P_4}{\sqrt{2}}\frac{u_1'}{r}\right)\left(\frac{u_0'}{\sqrt{2}r}\right)P_4{}^0r^2\sin\theta d\theta d\phi=\frac{4}{9}u_0'u_1'. \quad (11)$$

The extra factor of 2 is due to the fact that there are two s electrons. The calculation of the extra potential in Eq. (2) is reduced to a single integral of $u_0'u_1'$.

The details for obtaining the angular form of the excited state wave function and the values of $\rho_{n,m}(r)$ are in the appendix. The results will be discussed here.

The values for $F(r)$ integrated over the $4f$ wave

[3] See J. O. Hirschfelder, C. F. Curtiss, and R. B. Bird, *Molecular Theory of Gases and Liquids* (John Wiley & Sons, Inc., New York, 1954), Chap. 12.

[4] R. M. Sternheimer, Phys. Rev. **115**, 1198 (1959) and the references quoted there.

[5] See L. Schiff, *Quantum Mechanics* (McGraw-Hill Book Company, Inc., New York, 1949), p. 150.

[6] E. C. Ridley, Proc. Cambridge Phil. Soc. **56**, 41 (1960).

[7] G. Burns, Phys. Rev. **115**, 357 (1959).

functions are listed in Table I. All the nonzero perturbations are calculated for Pr^{+3} for the B_4^0, and $B_6^{0,6}$ perturbation. As can be seen, the results compared to the $4f$ expectation values are small. Wave functions without exchange were used for the calculations since they are the only complete set available.[6] The inclusion of exchange tends to contract the outer regions of the ion. Since the values of $\langle F(r)\rangle$ are negligible compared to the $\langle r^n\rangle$ values a small amount of contraction should not significantly alter the result. Several values of $F(r)$ were calculated for Tm^{+3} to see effect for a smaller ion. The results can be seen in Table I. The $F(r)$ values are reduced in just about the same ratio as the $\langle r^n\rangle$ values are reduced.

The calculation of the effect of the B_2^0 perturbation is more difficult for a technical reason. The excited state wave functions that have nonzero matrix elements with the $5s$ and $5p$ ground states will have nodes. This makes it more difficult to solve Eq. (5), at least by the method used here. There is no reason to expect anything very different to happen in the B_2^0. Judd[8] has calculated the shielding effect for the hydrogen atom and has shown that the effect is basically the same for $n=2$, 4 and 6 potentials. The only difference in the hydrogen case is that the shielding is larger for smaller n. However, there is a possibility for something unexpected to happen due to the normalization of the excited-state wave function to the ground state. For example, the B_2^0 term will connect $5p\rightarrow f$ and $5p\rightarrow p$. The p state from the latter perturbation must be made orthogonal to the ground $5p$ state. It is this orthogonalized excited p state that gives a large contribution to the antishielding factor[9] that is of importance in interpreting nuclear quadrupole resonance data. On the other hand, this special wave function has just its normal importance in the calculation of the quadrupole polarizability of the electron shells. Thus, it is of interest to see if the orthogonalization produces any large effects.

To do this, and in light of the difficulty experienced in obtaining these ψ_1's here it was decided to make use of the extensive wave functions (orthogonalized when required) that have been calculated in connection with antishielding and quadrupole polarizability calculations.[10] The perturbation for these problems is of the same form as the B_2^0 perturbation. Thus, if the proper u_1''s are known one need only do the radial integrations in Eq. (2) to determine $F_{2,0}(r)$. The wave functions used are these calculated by Sternheimer[10] for K^{+1}. they are calculated starting with ground-state wave functions that were calculated with exchange. Using these wave functions, $F_{2,0}(r)$ was calculated and its expectation value is taken over a normalized nodeless function that has about the same ratio of expectation values to the $3p$ as the Pr^{+3} $4f$ to $5p$ so that a somewhat reasonable comparison could be made between the $\langle F(r)\rangle$ for $n=2$, 4, and 6. The results for $n=2$ were also integrated over several other similar functions with little change in the results as given in Table I.

TABLE I. The expectation values of $F(r)$ over $4f$ wave functions for the B_4^0 and B_6^0 terms are given along with $\langle r^n\rangle$ of the $4f$ wave functions (all in atomic units). The wave functions used are those calculated by Ridley (see reference 6). For the B_2^0 perturbation the wave functions for K^{+1} are used as described in the text. (The shielding for the B_6^6 terms is smaller than the B_6^0 term by a factor of 3 for $s\rightarrow i$ and 84/52 for $p\rightarrow j$.)

Type of perturbation	Function	$-\langle F(r)\rangle$
B_4^0	Pr $5s\rightarrow g$	+0.09923
B_4^0	Pr $5p\rightarrow f$	−0.01087
B_4^0	Pr $5p\rightarrow h$	+0.16414
$\langle r^4\rangle=5.341$		$\Sigma=+0.2525$
B_6^0	Pr $5s\rightarrow i$	+0.1058
B_6^0	Pr $5p\rightarrow h$	+0.4448
B_6^0	Pr $5p\rightarrow j$	+0.1410
$\langle r^6\rangle=39.58$		$\Sigma=+0.6916$
B_4^0 ($\langle r^4\rangle=1.570$)	Tm $5s\rightarrow g$	+0.03271
B_6^0 ($\langle r^6\rangle=7.301$)	Tm $5p\rightarrow j$	+0.02923
B_2^0	K $3s\rightarrow d$	+0.1218
B_2^0	K $3p\rightarrow p$	−0.1265
B_2^0	K $3p\rightarrow f$	+0.1282
$\langle r^2\rangle=1.017$		$\Sigma=+0.1235$

The expectation values of $F(r)$ appear to increase as n increases, but at a slower rate than the increase of $\langle r^n\rangle$. Thus, the percentage effect is largest for $n=2$ as suggested from the hydrogen calculation. For B_2^0 the effect of orthogonalization in the $3p\rightarrow p$ is interesting in that it is of opposite sign from the other contributions but here there is no large effect as there is in calculating the antishielding factor. To see if the opposite sign is usual for the orthogonalized excited state wave function, the calculation of $F_{2,0}(r)$ was also performed for Cu^{+1} considering all the B_2^0 type perturbations from the ground $3d$ as well as $3s$ and $3p$ states. Again the excited-state wave functions have been calculated by Sternheimer[10] and the expectation value of $F_{2,0}(r)$ was taken over the $3d$ ground-state wave function ($\langle r^2\rangle=1.284$ a.u.^{2}). This is also of interest in the problem of calculating the zero-field splitting, D, in the spin-Hamiltonian. Again a cancellation is observed. (The $3d\rightarrow s$, $3d\rightarrow d$, and $3d\rightarrow g$ contributions are, respectively, +0.05852, −0.1462, and +0.07933 for a total of −0.0083. The $3s\rightarrow d$, $3p\rightarrow p$, and $3p\rightarrow f$ contributions are, respectively, +0.02711, −0.06297, and +0.03212 for a total of −0.0037.)

Thus, because $\langle F(r)\rangle$ increases with n at a slower rate than the increase of $\langle r^n\rangle$ with n the shielding effect is largest for $n=2$. However, the size of the shielding effects are small $\approx 12\%$, 5%, and 2% for $n=2$, 4, and 6, and there are no large effects as experienced in the field-gradient antishielding factor. These effects are

[8] B. R. Judd, Proc. Roy. Soc. (London) **A251**, 134 (1959).
[9] H. M. Foley, R. M. Sternheimer and D. Tycko, Phys. Rev. **93**, 734 (1954); R. M. Sternheimer and H. M. Foley, *ibid.* **102**, 731 (1956); R. M. Sternheimer, *ibid.* **84**, 244 (1951).
[10] R. M. Sternheimer, Document No. 6044-ADI Auxiliary Publications Project, Photoduplication Service, Library of Congress, Washington 25, D. C.

most probably a good deal smaller than the accuracy of the $\langle r^n \rangle$ values considering that the effect of the crystalline surrounds are not taken into account (see Appendix II). Also one cannot calculate the $B_n{}^m$ coefficients accurately (see Sec. IV).

LATTICE SUM ($B_n{}^m$) CALCULATIONS

If the shielding effects are small one should be able to calculate the $B_n{}^m$ coefficients by performing the proper lattice sums for the various lattices. This is done for several lattices that typically accept rare-earth ions and several that typically accept the iron series ions.

The quantities calculated for the various lattices are

$$\begin{aligned} C_2{}^0 &= \textstyle\sum_i j_i(3\mu_i{}^2-1)/r_i{}^3, \\ C_4{}^0 &= \textstyle\sum_i j_i(35\mu_i{}^4-30\mu_i{}^2+3)/r_i{}^5, \\ C_6{}^0 &= \textstyle\sum_i j_i(693\mu_i{}^6-945\mu_i{}^4+315\mu_i{}^2-15)/r_i{}^7, \\ C_6{}^6 &= \textstyle\sum_i j_i(1-\mu_i{}^2)^3 \cos 6\phi_i/r_i{}^7, \end{aligned} \tag{12}$$

where the sum is over all the i ions in the lattice each with a charge, j_i, at a distance r_i from the origin and u_i is cosine of the angle between the symmetry axis and r_i ($\mu_i = \cos\theta_i$). The numerical factors that relate the $C_n{}^m$'s to the $B_n{}^m$'s need not be discussed in this section since they are the same for any ion, rare earth or iron series.

The values calculated for these fairly typical and often used lattices are in Table II. For the purposes of this section, it is only necessary to look at 1(a)–5(a); the (b) (c), and (d) will be discussed in the next section. The crystal field parameters ($\propto \langle r^n \rangle C_n{}^m$) for a number of rare-earth ions in the first two lattices [1(a)—$LaCl_3$ and 2(a)—ethylsulfate] have been measured and x-ray data exist[11,12] so that the lattice sums, $C_n{}^m$, were calculated. The last three lattices (3–5), or very similar ones, have been used as hosts to measure a number of iron series ions. The rare earth in the $LaCl_3$ and ethylsulfate has nine nearest neighbors (9 Cl or 9 H_2O's) while the iron series ions have six. One must consider several important details to actually do the lattices sums, such as how to distribute the charge over the H_2O's, etc., the positions of the hydrogens, and the sensitivity of the sums to the x ray and charge distribution parameters. These details will be discussed more fully in the next section where a detailed numerical comparison with experimental rare-earth crystal field parameters will be made. In this section principally the differences between the rare-earth lattices and the iron series lattice is of interest.

One of the first things to notice in Table II is that the iron series lattices (3a–5a) have crystal fields that are larger than those in the rare earth lattices (forgetting about $C_2{}^0$ for the moment). This comes about for several reasons, but whatever the reasons, the rare earths see smaller crystal fields than the iron series ions. Also the crystal field splitting is determined by the product $\langle r^n \rangle C_n{}^m$ and the iron series ions have $\langle r^n \rangle$'s $\approx$ two times larger than the corresponding rare-earth ions. (For values of $\langle r^n \rangle$ for the iron series ions see the Appendix and for the rare-earth ions see a paper by Freeman and Watson[13]. The values for $\langle r^4 \rangle$ for Ti^{+3} to Cu^{+3} are 7.1 to 1.6 and Ce^{+3} to Er^{+3} are 3.4 to 1.2.[14] For $\langle r^6 \rangle$ they are 43 to 5.5 and 21 to 4, respectively, all in atomic units.) Thus, the crystal field splittings of the $4f$ electrons in the rare-earth ions are small because the crystal fields are small. The values of the spin-orbit coupling (s.o.) also favors the importance of the crystal field over s.o. in the iron series ions while the reverse is true in the rare earths; the s.o. parameters, ζ, for Ti^{+3} to Cu^{+3} are[15] 155 cm^{-1} to 875 cm^{-1} and for Ce^{+3} to Yb^{+3} are[16] 640 cm^{-1} to 2940 cm^{-1}.

It should also be pointed out that in the iron series ions there is a strong tendency for the ions in the second half of the group to be divalent. Thus, Co^{+2}, Ni^{+2}, and Cu^{+2} are the usual configurations rather than the $+3$ configuration. The $+2$ state will further increase the $\langle r^n \rangle$ values and decrease the s.o. parameters for these ions over those values listed above, again causing the crystal fields to be still more important in the iron series ions than the spin-orbit coupling.

Before the next section, in which numerical comparisons are made between the crystal field parameters calculated above for the rare earths and those obtained by fitting energy levels, it is appropriate to make several comments. In the iron series ions the large important crystal field parameter is the cubic crystal field parameter (approximately proportional to $\langle r^4 \rangle C_4{}^0$). It has been the subject of a considerable amount of theoretical and experimental work. One of the findings is that the point charge lattice sum does not give good agreement with the experimental $10Dq$ values. Various calculations have been performed to find out why.[17] It appears that important contributions to $10Dq$ arise from covalent bonding of the magnetic $3d$ electrons. This is possible because the $3d$ electrons in the iron series ions are the outer electrons and they can intimately mix with the neighboring ions. One finds that the covalent effects are bigger than the point charge effects in the iron series ions. Thus, the cubic crystal field in the iron series ions is actually larger than one would calculate from $C_4{}^0$ as listed in the table. This type

[11] D. R. Fitzwater and R. E. Rundle, Z. Krist. **112**, 362 (1959).
[12] W. H. Zachariasen, J. Chem. Phys. **16**, 254 (1948).
[13] A. J. Freeman and R. E. Watson, Phys. Rev. **127**, 2058 (1962). I am indebted to these authors for sending me their manuscript prior to publication.
[14] Values of $\langle r^n \rangle$ for the $4f$ wave functions are those from reference 13 since the wave functions were calculated with exchange. These values will be used whenever possible. However, since the only complete set of wave functions $5s^2p^6$, etc., for a single rare earth are those in reference 6, $\langle F(r) \rangle$ is compared to $\langle r^n \rangle$ of the $4f$ wave functions computed there.
[15] See T. M. Dunn, Trans. Faraday Soc. **57**, 1441 (1961).
[16] See B. Bleaney, Proc. Phys. Soc. (London) **A68**, 937 (1955).
[17] For a short review and references to the original work, see S. Sugano, J. Appl. Phys. **33**, 303 (1962).

TABLE II. Values for the lattice sums of Eq. (12) for several lattices.

	C_2^0 (10^{+14} esu/cm^3)	C_4^0 (10^{+30} esu/cm^5)	C_6^0 (10^{+46} esu/cm^7)	C_6^6 (10^{+43} esu/cm^7)
1(a)—$LaCl_3$[a] ($c/a=0.58463$)	+0.2918	+0.2605	+0.3250	−9.721
1(b)—UCl_3 ($c/a=0.5805$)	+0.3070	+0.2845	+0.3390	−10.18
1(c)—$GdCl_3$ ($c/a=0.55752$)	+0.4056	+0.4048	+0.3667	−11.43
1(d)—$LaCl_3$ maximum	+0.6649	+0.3390	+0.4213	−15.03
1(d)—$LaCl_3$ minimum	−0.06319	+0.1159	+0.2623	−6.890
2(a)—Er ethylsulphate[b] (Er E.S.)	−0.2773	+0.4875	+0.5093	−18.67
2(b)—$_{59}$Pr E.S. (nearest O's only)	−0.3353	+0.4030	+0.3477	−13.56
2(c)—$_{68}$Er E.S. (nearest O's only)	−0.3604	+0.4935	+0.4902	−18.55
2(d)—Y E.S. (nearest O's only)	−0.3893	+0.5065	+0.4663	−16.83
3(a)—Fe_2O_3[c]	+0.3063	+4.130	−2.802	−208.5
4(a)—$MgAl_2O_4$[d] ($u=0.387$)	+0.1918	+6.649	−3.674	−116.8
5(a)—K Cr alum[e] (nearest H_2O's only)		+1.608	−2.156	−49.41

[a] The atomic position coordinates for UCl_3 are used for all the lattices (see reference 12). The c and a values can be found in references 12 and 21. In 1(d) the x and y describing the coordinates of the Cl^{-1} were varied by ± 0.02 to obtain a maximum and minimum for the sums.
[b] The x-ray data of Fitzwater and Rundle are used (see reference 11).
[c] The x-ray data of D. E. Cox and G. Shirane (private communication) are used. (Fe parameter $u=0.355$, O parameter $x=0.552$, $\alpha=55°\,17'$, and $a=5.424$ Å).
[d] G. E. Bacon, Acta Cryst. **5**, 684 (1952).
[e] G .E. Bacon and W. E. Gardner, Proc. Roy. Soc. (London) **246**, 78 (1958). C_2^0 is not included since other ions will make important contributions to it.

of covalent bonding is expected to be vastly reduced for $4f$ electrons in rare earths since the $5s^2p^6$ electrons are now the outer ones. Thus, the C_4^0's for the rare earths should be reasonable and the C_4^0 type of crystal fields are even larger for the iron series ions than calculated as in Table II. Very probably the situation would be similar for the iron group C_6^0 type of crystal fields.

COMPARISON WITH RARE-EARTH CRYSTAL FIELDS

In this section a comparison is made between the crystal field splitting parameters that are found for rare-earth energy levels and those calculated from the lattice sums. For convenience, the crystal field is taken in the form as given by Elliott and Stevens.[18]

$$V=A_0^0+A_2^0(3z^2-r^2)+A_4^0(35z^4-30r^2z^2+3r^4)+A_6^0(231z^6-315r^2z^4+105r^4z^2-5r^6)+A_6^6(x^6-15x^4y^2+15x^2y^4-y^6). \quad (13)$$

Only these terms are needed for the $LaCl_3$ and ethylsulfate crystals.

By considering optical or specific heat and resonance data, they have been able to fit the energy levels with the four crystal field parameters, i.e., $\langle r^2\rangle A_2^0$, $\langle r^4\rangle A_4^0$, $\langle r^6\rangle A_6^0$, and $\langle r^6\rangle A_6^6$. The relations between the lattice sums calculated and listed in Table II and the A_n^m's are

$$A_2^0=-eC_2^0/4, \qquad A_4^0=-eC_4^0/64, \qquad A_6^0=-eC_6^0/768, \qquad A_6^6=-231eC_6^6/512. \quad (14)$$

where $e=4.8029\times10^{-10}$ esu. The minus sign arises because it is an electron in the potential of the lattice. The values of $\langle r^n\rangle$ of the $4f$ electrons are obtained from the recently calculated wave function for rare-earth ions.[6,13] The $4f$ wave functions calculated by Freeman and Watson with exchange are used here.[13]

Before discussing the computed numerical values for the crystal field parameters a number of problems that arise when the lattice sums are calculated are discussed. This bears on the sort of agreement one should expect.

A. Lattice Sum Problems

In order to calculate lattice sums as listed in Table II a number of problems arise. Some of these problems are extrinsic in the sense that better x-ray or thermal expansion data, for example, would solve them, but some of the problems are of a more intrinsic nature.

One is faced with the extrinsic problem of obtaining good x-ray data for the crystal. Then, especially in the case of the ethylsulfates (E.S.), one must divide up the charge, i.e., exactly where is the charge on the SO_4^{-2} ion or the H_2O molecule? The lattice sums are point charge sums so one must pick out a point at which to place the charge. Dipole, etc., moments can be taken care of by a charge-distance arrangement approximating the moment. For example, there are nine H_2O molecules immediately surrounding the rare-earth ions in E.S. They have no charge but they do have large dipole moments. In order to do the lattice sums the dipole moment is approximated by a charge of $-\eta$ on the oxygen atoms and $+\eta/2$ on each of the hydrogen atoms with $\eta=0.6$ so that the value of the dipole moment in gaseous H_2O approximately is reproduced.[19] Also, the positions of the hydrogen atoms must be guessed at since x-ray work will not give their positions.[11] This is done by

[18] R. J. Elliott and K. W. H. Stevens, Proc. Roy. Soc. (London) Å**219**, 387 (1953). Also references to the earlier papers in this series are given there.

[19] See Chap. 13 in reference 3.

locating them 1.02 Å along the most probably hydrogen bond direction. Both this hydrogen location scheme and the η value had been previously used with some success.[20] For the E.S. lattice, one must also distribute the charge for the ethylsulfate ion, $(C_2H_5SO_4)^{-1}$. This is done by assigning a charge of -2 to the S position in the SO_4 group and a charge of $+1/2$ to each of the C atoms. As will be seen, the effect on the A_4^0 and $A_6^{0,6}$ sums is not important.

Fortunately, Fitzwater and Rundle[11] have published detailed x-ray results on the crystal structure of Er, Y, and Pr ethylsulfates and their structure parameters are used. The situation is not as simple for the $LaCl_3$ structure. The values of the c and a dimensions in this hexagonal cell have been given for $LaCl_3$ and many of its isomorphous compounds.[12,21] However, the atomic position parameters, which describe the position of the ions in the cell, have only been given for UCl_3.[12] To do the calculations, the UCl_3 parameters were used with values of c and a appropriate to La, U, and Gd trichloride. The results for C_n^m appear in Table II as 1(a)–1(c), respectively. Finally, the x-ray position parameter of the Cl^{-1} ions (the error in this case is large) is varied within approximately the given experimental $(x, y = \pm 0.02)$ error to see the effects on the C_n^m results. The results are given in 1(d) of Table II for c and a corresponding to $LaCl_3$ and as can be seen the C_n^m's vary considerably, in fact C_2^0 changes sign. Accurate x-ray data for the trichlorides would be very helpful.

Thermal expansion and the change of the x-ray position parameters with temperature are also important to bear in mind. Many of the optical, etc., data that go into determining the crystal field splitting parameters have been measured at low temperatures. The x-ray data are room-temperature data. Temperature changes in the position parameters, judging from 1(d), can have some noticeable effects. The thermal contraction of the crystal will also effect the C_n^m's since the internuclear distances will be smaller but more important, the shape (c/a) of the unit cell will change. Again, x-ray data could elucidate these points.

The sensitivity of the C_2^0's to the x-ray coordinates is an old problem since C_2^0 is just the field gradient q that one is concerned with in nuclear quadrupole coupling measurements. The sensitivity of q to x-ray coordinates and convergence of the lattice sum has been discussed previously.[22] As can be seen in 1(a)–1(d) of Table II, C_2^0 varies considerably with changes in the shape of the unit cell and with changes in the atomic position coordinates.

As mentioned in the previous paragraph, the convergence of the C_2^0 lattice sum is not rapid and care must be taken in evaluating the sum. The convergence for the other sums is rapid. However, more than just nearest neighbors are required to give reasonably accurate values. Table III is a breakdown of the contributions to the C_n^m's from the various ions or groups. Each contribution for each ion is actually the sum out to several lattice constants but, especially for $n \geqq 4$, only the contribution with the smallest r_i is important. As can be seen all the ions can give important contributions to C_2^0. However, the other C_n^m's are still influenced by the next neighbor ions. For example, the contribution from La^{+3} to the C_4^0 is about as big as the resultant Cl^{-1} contribution. The contributions from the iron series ions are more evenly spread among all the ions. Only the nearest-neighbor oxygen atoms of the H_2O molecules make substantial contributions to C_4^0 and $C_6^{0,6}$ in the ethylsulphates. Thus, only these oxygen contributions were calculated for Y E.S. and Pr E.S. and they appear as 2(d) and 2(b) in Table II.

Another problem in comparing the calculated crystal field splittings with those obtained by fitting optical, etc., levels is that some of the spectroscopy is done on the rare earth diluted by the appropriate salt, i.e., approximately 1% Gd in $LaCl_3$. Thus, the problem arises: Does the Gd^{+3} see the crystal fields it would in $GdCl_3$, or the fields appropriate to $LaCl_3$, or some average? If the calculations, as made in Table II, are appropriate (which is open to question until the x-ray work is done), the various fields are somewhat different even for these isomorphous compounds. Care must be taken if one obtains a set of crystal field splitting parameters from dilute and nondilute crystals. However, the problem of which field the ions would see should be easy to find out experimentally. Some work has been done along these lines for the iron series ions.[23]

The last problem discussed in this section is very important and yet probably not tractable. The C_6 lattice sums are $\approx 1/R^7$, where R is the internuclear distance between the rare-earth ion and the nearest-neighbor ion (Cl^{-1} for $LaCl_3$ or O for the E.S.). Now the lattice sums are computed for point charges. Thus, it is assumed that the Cl^{-1} ion is spherical and can be replaced by a charge at its center. One could go further and calculate the electric field at the Cl^{-1} site and then the induced dipole moment, etc. This induced dipole moment would also contribute to C_6, etc. However, this is really not enough since the Cl^{-1} ion can not be spherical. It overlaps the La^{+3} and other Cl^{-1} ions. These effects might be able to be taken care of in a simple electrostatic manner by considering various moments. However, the point of observation of the fields is not large compared to the radii of the ions. Thus, the use of higher moments localized at the nucleus of the Cl^{-1} ion becomes limited. Consider some sort of distortion in the Cl^{-1} ion out near its ionic radius along the internuclear line joining the Cl^{-1} and rare-earth ions. If this distortion can be taken care of electrostatically,

[20] G. Burns, Phys. Rev. **123**, 1634 (1961).
[21] D. H. Templeton and C. H. Dauben, J. Am. Chem. Soc. **76**, 5237 (1954).
[22] R. Bersohn, J. Chem. Phys. **29**, 326 (1958).
[23] G. Burns and W. J. Nicholson, "International Conference on Magnetic and Electric Resonance and Relaxation," Eindhoven, 1962 (to be published).

TABLE III. The contributions to C_n^m are listed from the various types of ions in the lattice. To actually obtain the C_n^m's one must multiply the numbers by the charge of the ion and the number of equivalent ions (both numbers are in parenthesis in the left-hand column) and divide by a^{n+1} (a is the unit cell dimension). [The origin is at La $(\frac{1}{3}, \frac{2}{3}, \frac{1}{4})$ and Fe(u,u,u).]

Lattice		C_2^0	C_4^0	C_6^0	C_6^6
$LaCl_3$					
La$(\frac{1}{3},\frac{2}{3},\frac{1}{4})$	$(+3e)$ (1)	15.36	244.4	4112	8.264
La $(\frac{2}{3},\frac{1}{3},\frac{3}{4})$	$(+3e)$ (1)	−5.729	−89.20	1916	−66.11
Cl $(x,y,\frac{1}{4})$	$(-1e)$ (3)	−15.51	317.2	−10581	679.1
Cl $(x,y,\frac{3}{4})$	$(-1e)$ (3)	+17.13	−581.9	−12614	137.0
$(x=0.375, y=0.292)$					
Er ethylsulfate					
O_6	$(-\eta)$ (3)	−150.3	15445	-2.316×10^6	1.545×10^5
O_7	$(-\eta)$ (6)	131.6	−22613	-1.705×10^6	0.3112×10^5
$(\eta=0.6e)$					
Fe_2O_3					
Fe (u,u,u)	$(+3e)$ (1)	−0.7005	19.28	−263.9	−10.97
Fe $(\bar{u},\bar{u},\bar{u})$	$(+3e)$ (1)	9.718	105.5	5347	−38.72
Fe $(\frac{1}{2}+u, \frac{1}{2}+u, \frac{1}{2}+u)$	$(+3e)$ (1)	2.509	−133.4	558.4	−22.75
Fe $(\frac{1}{2}-u, \frac{1}{2}-u, \frac{1}{2}-u)$	$(+3e)$ (1)	−10.35	149.7	−404.8	−184.4
O $(x, \frac{1}{2}-x, \frac{1}{4})$	$(-2e)$ (3)	9.204	−398.8	−3372	128.1
O $(\bar{x}, \frac{1}{2}+x, \frac{3}{4})$	$(-2e)$ (3)	10.31	−203.5	19420	709.3
$(u=0.355, x=0.552, \alpha=55°\,17')$					

it would be an effect $\approx(2.8/1.0)^7$ times as large as a similar effect occurring at the center of the Cl^{-1} ion (i.e., taking the ionic radii of Cl^{-1} on the rare earth to be 1.8 Å and 1 Å, respectively). This is a large number and very small effects can thus be important. These distortions, etc., effects probably occur readily in the Cl^{-1} and O atom in the H_2O molecule since the molecule is easily polarizable. Another similar and important consideration for the H_2O, molecule is the representation of it by a charge of $-\eta$ on the O and $+\eta/2$ on each of the hydrogens. This seems reasonable if the sum converges slowly enough so that every time an $-\eta$ charge gives a contribution, the two $+\eta/2$ charges also are important so that the idea of the dipole is meaningful. This occurs for the C_2^0 sum but does not for the sums for larger n where the nearest O is much more important than the nearest hydrogens. Thus, the explicit C_n^m result depends sensitively on the method of distributing the charge on the H_2O molecule.

The above considerations give some indication of the problems involved in calculating the lattice sums. Clearly very good agreement between the calculated parameters, $\langle r^n\rangle C_n^m$, and those obtained by fitting various kinds of experimental data would not be expected. However, the comparison will be made and discussed in the next section. Still a comparison between the C_n^m's calculated for the rare earth lattices and the iron series lattice should be much more meaningful. Many of the above difficulties will tend to cancel out and the qualitative aspect of Table II, namely, that the rare earths see smaller crystal fields than the iron series ions, will remain.

B. $\langle r^n\rangle A_n^m$ Values

To calculate the crystal field splitting parameters, $\langle r^n\rangle A_n^m$, for the trichlorides and the E.S.'s the C_n^m's of Table II are used. The relations between the C_n^m's and the A_n^m's are in Eq. (14). The $4f\langle r^n\rangle$ values used are those calculated by Freeman and Watson for the rare earth ions with exchange.[13] To simplify matters the $\langle r^2\rangle$, $\langle r^4\rangle$, and $\langle r^6\rangle$ used are those for Ce^{+3}. Their values are[13] 1.200, 3.455, and 21.226, respectively (in atomic units, 1 a.u.=0.52917 Å). Values for the other rare earths, i.e., those with higher Z, are smaller (lanthanum contraction). The results for the calculated values of $\langle r^n\rangle A_n^m$ are listed in Table IV along with the calculated ratio[24] A_6^6/A_6^0.

One would like to compare these calculated values to those obtained by fitting the optically observed energy levels, etc. To do this, a certain amount of judgement is required to pick good fits to the observed energy levels, as some of the earlier fitting procedures gave very inaccurate values. References to the original papers of some of the more recent and undoubtedly more accurate fits can be found in footnote.[25] In fitting the energy levels only the product of $\langle r^n\rangle$ with A_n^m is involved ($\langle r^n\rangle A_n^m = V_n^m$) and not each separately. The values of V_n^m obtained do not vary greatly for the various rare-earth ions in each of these two lattices. Thus, typical values are listed so that a comparison can be made with $\langle r^n\rangle A_n^m$ in Table IV. The V_n^m values are in the usual cm^{-1} units.

	V_2^0	V_4^0	V_6^0	V_6^6	A_6^6/A_6^0
Trichlorides	+80	−35	−25	+260	−10.5
Ethylsulfates	+120	−50	−30	+420	−14

In comparing these values with the calculated values in Table IV one notices that the signs are in all cases in agreement except for the $LaCl_3$ A_2^0 value. This is not

[24] Also see C. A. Hutchison and E. Wong, J. Chem. Phys. **29**, 754 (1958).

[25] See references to the original literature in footnote 13.

TABLE IV. Values of $\langle r^n\rangle A_n{}^m$ are given in cm^{-1}. The $A_n{}^m$'s are defined in the usual way (see reference 18) and the $\langle r^n\rangle$ values used are those of Freeman and Watson (see reference 13) for Ce^{+3}.

	$\langle r^2\rangle A_2{}^0$ (cm^{-1})	$\langle r^4\rangle A_4{}^0$ (cm^{-1})	$\langle r^6\rangle A_6{}^0$ (cm^{-1})	$\langle r^6\rangle A_6{}^6$ (cm^{-1})	$A_6{}^6/A_6{}^0$
$LaCl_3$ ($c/a=0.58463$)	−592.6	−26.66	−4.771	+49.44	−10.3
UCl_3 ($c/a=0.5805$)	−623.5	−29.12	−4.977	+51.79	−10.4
$GdCl_3$ ($c/a=0.55752$)	−823.7	−41.44	−5.383	+58.15	−10.8
$LaCl_3$ maximum	−1348	−34.71	−6.185	+76.44	−12
$LaCl_3$ minimum	+128.3	−11.87	−3.864	+35.04	−9.1
Er ethylsulphate (Er E.S.)	+563.2	−49.93	−7.477	+94.95	−12.7
$_{59}Pr$ E.S. (nearest O's only)	+681.0	−41.25	−5.104	+68.98	−12.5
$_{68}Er$ E.S. (nearest O's only)	+732.0	−50.52	−7.196	+94.34	−13
Y E.S. (nearest O's only)	+790.6	−51.85	−6.846	+85.59	−13

surprising since the $A_2{}^0$ lattice sum is sensitive to the atomic position parameters [see 1(d)] and these parameters are only roughly given for UCl_3 and assumed to approximately hold for $LaCl_3$. Also, the magnitudes of the calculated values in Table IV are smaller than the $V_n{}^m$'s, especially for $V_6{}^{0,6}$. It is again difficult to say anything about the magnitude of $\langle r^2\rangle A_2{}^0$ for the trichlorides for the reasons mentioned above. For $n=4$ and 6 only the nearest-neighbor oxygens contribute significantly to $A_n{}^m$ for the ethylsulfates. However, all the ions contribute to $A_2{}^0$ ($\propto$ field gradient). Its value is sensitive to the position of the hydrogen atoms of the H_2O molecules. Keeping the same η and H—O distance (1.02 Å) one can move the hydrogens about, particularly the hydrogens associated with O_7, and reduce $A_2{}^0$ to ≈ 0. Thus, again one cannot expect good agreement between the parameters obtained from optical data and the lattice sums for $V_2{}^0$. The calculated ratios of $A_6{}^6/A_6{}^0$ are in fairly good agreement with those obtained by fitting energy levels.

It should again be pointed out that the $\langle r^n\rangle$ values used in Table IV are those for Ce^{+3} which is the biggest of the rare earths. For example, Freeman and Watson find that $\langle r^4\rangle$ decreases by a factor of 2.5 in going from $_{59}Pr^{+3}$ to $_{68}Er^{+3}$ and $\langle r^6\rangle$ decreases by 3.9, while the lattice sums $C_4{}^0$ and $C_6{}^0$ increase by a factor of 1.2 and 1.4 in going from Pr to Er E.S. (see Table II). (Due to the lack of x-ray data for the trichlorides one cannot say in detail how the lattice sums will vary.) The experimental $V_n{}^m$'s (for $n=4$ and 6) tend to decrease slightly with increasing atomic number. Thus, the situation appears to be: The calculated $\langle r^n\rangle A_n{}^m$ ($n=4$ and 6) tend to a smaller than the $V_n{}^m$'s obtained by fitting the optical data, and the discrepancy gets larger with increasing atomic number due to the fact that the $\langle r^n\rangle$ decrease at a much faster rate than the $C_n{}^m$'s increase. It should not be too surprising that there is a lack of detailed numerical agreement in light of the difficulties in calculating the $C_n{}^m$'s discussed in the previous section. Particularly important should be the effects of nonsphericalness in the outer regions of the polarizable negative ions or H_2O groups. As discussed in the last section, the $1/R^{n+1}$ factor weights these regions very heavily for $n=4$ and 6. It should also be pointed out that one has the usual problems with the expectation values of r^n. The $4f$ wave function is an inner wave function but it does have a long tail. Even though essentially all of its charge density is at distances smaller than the ionic radius of the ion, the small outer portions of the charge contribute heavily to the higher moments, for example, more than 50% of the contribution to $\langle r^6\rangle$ comes from regions outside the ionic radius. This is not an unusual situation for ions in solids but should be borne in mind. (See Appendix II.)

The $C_2{}^0$ type of crystal field is not very important in determining energy levels in either the rare earths or the iron groups. However, $C_2{}^0$, as defined here, is just the lattice contribution to the field gradient, q, that is of interest for interpreting nuclear quadrupole coupling constants, eQq/h. It can be seen that the rare-earth lattices have field gradients $\approx$ iron series lattices, even though one usually considers the latter as slightly distorted from cubic symmetry while the rare-earth lattices considered here bear little resemblance to cubic symmetry. Still the various contributions from the various ions in these rare-earth lattices tend to cancel, as in the iron series lattices, with a resultant small value for q. Since the antishielding factor associated with the lattice contributions to q will be large for the rare-earths ions, their effects will be noticed in interpreting eQq/h results.[26]

SUMMARY

(1) It is often said that in rare-earth ions the $4f$ electrons are shielded from the crystal field by the outer $5s^2p^6$ electrons. Using the usual ionic, electrostatic ideas a quantamechanical calculation of the shielding is performed. It is shown that the shielding is unimportant.

(2) Then the crystal fields in several typical rare earth and iron series lattices are calculated and compared (i.e., the $B_n{}^m$ lattice sums in the crystal field, $\sum B_n{}^m r^n Y_n{}^m$, are calculated). The crystal fields in the rare-earth lattices are 3 to 10 times smaller than the

[26] E. G. Wikner and G. Burns, Phys. Letters 2, 225 (1962).

iron series lattices mainly because the rare-earth ions are physically larger than the iron series ions ($B_n^m \propto 1/R^{n+1}$). Thus, the $5s^2p^6$ electrons cause the rare earths to be large ions and they, in a sense, mechanically shield the $4f$ electrons. Also, the crystal field splittings are $\propto \langle r^n \rangle B_n^m$ and $\langle r^n \rangle$, for positive n, for the $4f$ electrons are approximately half as large as the corresponding values for the $3d$ electrons. On the other hand, the spin orbit coupling parameters for the rare earths are approximately twice as large as those of the iron series ions. Thus, the predominance of the spin orbit coupling over the crystal field splitting in the rare-earth ions comes about in a straightforward manner. (Vice versa for the iron series ions.)

(3). The sensitivity of the B_n^m lattice sums to the x-ray and charge-distribution parameters for the rare-earth lattices is investigated. As expected the B_2^0 is sensitive to these parameters. Thus, one can say little when comparing these calculated lattice sums to the values obtained by fitting optical energy levels. The $n=4$ and 6 sums suffer much less from the sensitivity but they could easily be effected by small charge distortions in the neighboring ions near the ionic radius of the rare earth. These effects will be heavily weighted since $B_n^m \propto 1/R^{n+1}$ and the convergence of these lattice sums is too rapid to average out these effects.

(4). A comparison between the calculated $\langle r^n \rangle A_n^m$'s ($\langle r^n \rangle$ from Freeman and Watson[13] and A_n^m, $\propto B_n^m$, calculated here) and those obtained by fitting the optical absorption data is made. Little can be said for $n=2$ for reasons mentioned above. For $n=4$ and 6 the calculated values tend to be small, particularly for $n=6$ although the ratio of A_6^6/A_6^0 is in good agreement with the optical fitting. Also agreement as one goes along the rare series, i.e., Ce to Yb, gets worse since the parameters obtained from optical fitting tend to decrease somewhat while the calculated A_n^m's increase somewhat (lanthium contraction) but the $\langle r^n \rangle$'s decrease at a much faster rate than the A_n^m's increase.

It is difficult to quantitatively tell how the A_n^m's will be affected by charge distortions near the ionic radius of the rare-earth ions as discussed above. However, one should also bear in mind, as discussed in the Appendix, that a large fraction of the contribution to $\langle r^6 \rangle$, etc., comes from a very small fraction of the $4f$ charge and could be easily altered in solids.

ACKNOWLEDGMENTS

It is a pleasure to acknowledge conversations with Professor R. Orbach, Dr. M. J. Freiser, Dr. G. J. Lasher, and Dr. W. V. Smith; programming assistance by N. J. Anthony; and a manuscript prior to publication from Dr. A. J. Freeman and Dr. R. E. Watson.

APPENDIX I

In this Appendix the method of finding the perturbed wave function and $\rho_{n,m}(r)$ is discussed.

The form of the crystal potential can be taken as

$$V(r\theta\phi)=\sum_{n=0}^{\infty}\sum_{m=-n}^{+n}\frac{(n-|m|)!}{(n+|m|)!}P_n^m(\mu) \times e^{-im\phi}r^n\Big[\sum_i j_i P_n^m(\mu_i)e^{im\phi_i}/R_i^{n+1}\Big] \quad \text{(A1)}$$

($\mu=\cos\theta$ and j_i is the charge on the ith ion). This is a convenient form since one can then use the recursion formulas for P_n^m which are a bit simpler than those for Y_n^m. Equation (A1) describes the potential in the space, where the rare-earth ion site is, due to a distribution of discrete charges around it. If the surrounding charge distribution is continuous there is just a trivial change in the square bracket in (Al).

If the potential in (A1) is used as a perturbation, one can obtain a first-order perturbed wave function, ψ_1, so that the total wave function is $\psi=\psi_0+\psi_1$. Then the charge density will essentially be $\psi_0^2+2\psi_0\psi_1+\psi_1^2$. In calculating shielding, etc., the ψ_0^2 part is of no interest and the ψ_1^2 is second order in the perturbation so only the $2\psi_0\psi_1$ term is considered. This will contain the numerical factors [the square bracket in Eq. (Al) $\propto B_n^m$] to the first power. The effect of the perturbation can be found by computing the additional potential in the space around the origin (rare-earth site) due to the distorted charge density of the rare-earth ion. This is given in Eq. (2), where $\rho_{n,m}$ is defined in Eq. (3). Note that $\rho(r\theta\phi)$ contains the square bracket to the first power so the extra potential can be written as $B_n^m Y_n^m F_{n,m}(r)$ if the initial perturbing potential were taken as $B_n^m Y_n^m r^n$. $F_{n,m}(r)$ is just the radial integral in the square bracket in Eq. (2) containing none of the numerical factors which are conveniently lumped in B_n^m.

An example will make this clearer. Consider the B_4^0 term as a perturbation on the s-state wave function. Then one can find the angular form of the excited-state wave function in a manner pointed out by Sternheimer.[4] The normalized angular part of the s wave function is $1/(2\pi)^{1/2}$ and the angular part of the perturbation is P_4^0. Thus, the angular part of the right-hand side of Eq. (4) is $P_4^0/(2\pi)^{1/2}$ which is a g-type wave function. Then r times the excited-state wave function is

$$r\psi_1=[P_4^0/(2\pi)^{\frac{1}{2}}]u'_{s\to g}, \quad \text{(A2)}$$

where $u'_{s\to g}$ is the u_1' that must be obtained by solving Eq. (5). The $\rho_{4,0}$ of Eq. (3) is

$$\rho_{4,0}=4\left\langle \frac{u_s'}{(2\pi)^{1/2}}\middle| P_4^0 \middle| \frac{P_4^0}{(2\pi)^{1/2}}u'_{s\to g}\right\rangle=\frac{4}{9}(u_s'u'_{s\to g}), \quad \text{(A3)}$$

where the extra factor of 2 is due to the fact that there are two electrons in the s state and u_s' is r times the radial part of the ground-state wave function.

In a similar manner, one can find $\rho_{4,0}$ for the ground-

state p_z wave functions:

$$\rho_{4,0}=4\left\langle\frac{\sqrt{3}}{2}\cos\theta\, u_p'\,|P_4^0|\frac{\sqrt{3}}{2}\left(\frac{4}{9}P_3^0u'_{p\to f}+\frac{5}{9}P_5^0u'_{p\to h}\right)\right\rangle$$

$$=(64/189)(u_p'u'_{p\to f})+(100/297)(u_p'u'_{p\to h}). \quad \text{(A4)}$$

For the four electrons in p_x and p_y states $[\frac{1}{2}\sqrt{3}(\sin\theta)u_p']$, one obtains

$$\rho_{4,0}=(16/63)(u_p'u'_{p\to f})+(40/99)(u_p'u'_{p\to h}). \quad \text{(A5)}$$

For the B_6^0 terms, adding up all the p_z and p_x and p_y contributions, one has

$$\begin{aligned}&\rho_{6,0}=(4/13)(u_s'u'_{s\to i}),\\ &\rho_{6,0}=(792/1859)(u_p'u'_{p\to h})+(84/169)(u_p'u'_{p\to i}).\end{aligned} \quad \text{(A6)}$$

For the B_6^6 terms one obtains

$$\rho_{6,6}=(4/39)(u_s'u'_{s\to i}),\quad \rho_{6,6}=(4/13)(u_p'u'_{p\to i}). \quad \text{(A7)}$$

The values of $\rho_{2,0}$ for the various excitations are directly related to the angular integrals used in calculating antishielding factors and quadrupole polarizabilities.[27]

$$\begin{aligned}&\rho_{2,0}=(4/5)(u_s'u'_{s\to d}),\\ &\rho_{2,0}=(24/25)(u_p'u'_{p\to p})+(36/25)(u_p'u'_{p\to f}).\end{aligned} \quad \text{(A8)}$$

In all the above cases u_1' is obtained from Eq. (5) as described in the text and

$$F_{n,m}(r)=\frac{1}{r^{n+1}}\int_0^r r_i^n\rho_{n,m}dr_i+r^n\int_r^\infty\frac{\rho_{n,m}}{r_i^{n+1}}dr_i. \quad \text{(A9)}$$

This $F_{n,m}(r)$ can be directly compared to r^n as in Table I.

APPENDIX II

In this Appendix values of $\langle r^n\rangle$ for the $3d$ ions are given and $\langle r^n\rangle$ values for the rare earths are discussed briefly. Watson has calculated the wave functions for several configurations of the iron series ions.[28] To compare $\langle r^n\rangle$ values between the rare earths and the iron series ions, values of $\langle r^n\rangle$ of the latter were computed and are listed in Table V. Also listed are values of $\langle r^n\rangle$ for several ions that might be useful for resonance purposes.

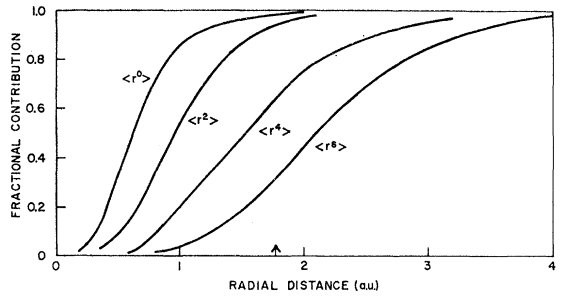

FIG. 1. A plot of the fractional contribution to $\langle r^n\rangle$ for the $4f$ wave function (see reference 13) of Gd^{+3}. All of the $\langle r^n\rangle$ values are normalized to unity.

TABLE V. Values of $\langle r^n\rangle$ are given for various iron series ions. (Results are in atomic units, i.e., 1 a.u.=0.52917 Å.) The wave functions, with exchange, calculated by Watson were used (see reference 28).

Ion (state)	$\langle r^{-3}\rangle$	$\langle r^2\rangle$	$\langle r^4\rangle$	$\langle r^6\rangle$
Ti^{+3} (^2D)	2.552	1.893	7.071	43.16
V^{+3} (^3F)	3.217	1.643	5.447	30.00
Ti^{+1} (^4F)	1.706	3.508	31.62	544.5
V^{+2} (^4F)	2.748	2.070	9.605	79.54
Cr^{+3} (^4F)	3.959	1.447	4.297	21.49
Mn^{+4} (^4F)	5.361	1.104	2.389	8.473
Cr^{+2} (^5D)	3.451	1.781	7.211	52.90
Mn^{+3} (^5D)	4.790	1.286	3.446	15.73
Cr^{+1} (^6S)	2.968	2.319	14.14	172.1
Mn^{+2} (^6S)	4.250	1.548	5.513	36.03
Fe^{+3} (^6S)	5.724	1.150	2.789	11.66
Co^{+4} (^6S)	7.421	0.9080	1.659	5.065
Fe^{+2} (^5D)	5.081	1.393	4.496	26.71
Co^{+3} (^5D)	6.699	1.049	2.342	9.055
Co^{+2} (^4F)	6.035	1.251	3.655	19.75
Ni^{+3} (^4F)	7.790	0.9582	1.971	7.058
Co^{+1} (^3F)	5.388	1.576	6.637	55.86
Ni^{+2} (^3F)	7.094	1.130	3.003	14.83
Cu^{+3} (^3F)	9.018	0.8763	1.662	5.525
Cu^{+2} (^2D)	8.251	1.028	2.498	11.32

Figure 1 is a plot for the contribution to the various $\langle r^n\rangle$'s as a function of radial distance (i.e., $\int_0^R\psi^*r^n\psi d\tau$ as a function of R). All the $\langle r^n\rangle$'s are normalized to 1. The plot is for Gd^{+3} using Freeman and Watson's wave functions[13] with exchange. Results are similar for the other wave functions. The arrow at 1.77 a.u. (1 a.u.=0.52917 Å) corresponds to the ionic radius of Gd^{+3}. As can be seen in the figure essentially all of the $4f$ charge ($\langle r^0\rangle$) is confined to regions within the ionic radius. On the other hand, a large percentage of the contribution to $\langle r^6\rangle$ comes from regions outside the ionic radius and from only a small fraction of the $4f$ charge. Thus, it is possible that the $\langle r^6\rangle$ values are not as accurately predicted from the Hartree-Fock wave functions as perhaps $\langle r^{-3}\rangle$ (90% of the contribution to $\langle r^{-3}\rangle$ for Gd^{+3} comes before 0.55 a.u.). This situation is quite normal for the outer electron shells of ions in ionic lattices. The point here is that even though the $4f$ electrons are not the outer electrons, still a good deal of the contribution to $\langle r^4\rangle$ etc., comes from regions outside the ionic radius.

[27] The angular integrals are just 1/2 those used in defining the quadrupole polarizability. See Eq. (101) of R. M. Sternheimer, Phys. Rev. **96**, 951 (1954).

[28] R. E. Watson, Phys. Rev. **118**, 1036 (1960); and Technical Report No. 12, "Solid State and Molecular Theory Group," Massachusetts Institute of Technology, 1959 (unpublished).